© 2018. Published by The Company of Biologists Ltd | Journal of Experimental Biology (2018) 221, jeb171967. doi:10.1242/jeb.171967

RESEARCH ARTICLE

Biochemical bases of growth variation during development: a study of protein turnover in pedigreed families of bivalve larvae (*Crassostrea gigas*)

T.-C. Francis Pan, Scott L. Applebaum, Christina A. Frieder and Donal T. Manahan*

ABSTRACT

Animal size is a highly variable trait regulated by complex interactions between biological and environmental processes. Despite the importance of understanding the mechanistic bases of growth, predicting size variation in early stages of development remains challenging. Pedigreed lines of the Pacific oyster (*Crassostrea gigas*) were crossed to produce contrasting growth phenotypes to analyze the metabolic bases of growth variation in larval stages. Under controlled environmental conditions, substantial growth variation of up to 430% in shell length occurred among 12 larval families. Protein was the major biochemical constituent in larvae, with an average protein-to-lipid content ratio of 2.8. On average, 86% of protein synthesized was turned over (i.e. only 14% retained as protein accreted), with a regulatory shift in depositional efficiency resulting in increased protein accretion during later larval growth. Variation in protein depositional efficiency among families did not explain the range in larval growth rates. Instead, changes in protein synthesis rates predicted 72% of growth variation. High rates of protein synthesis to support faster growth, in turn, necessitated greater allocation of the total ATP pool to protein synthesis. An ATP allocation model is presented for larvae of *C. gigas* that includes the major components (82%) of energy demand: protein synthesis (45%), ion pump activity (20%), shell formation (14%) and protein degradation (3%). The metabolic trade-offs between faster growth and the need for higher ATP allocation to protein synthesis could be a major determinant of fitness for larvae of different genotypes responding to the stress of environmental change.

KEY WORDS: Protein synthesis, Development, Larvae, Pacific oyster, Pedigreed lines, Metabolic trade-offs

INTRODUCTION

Quantitative bioenergetic frameworks are required to understand how organisms allocate cellular energy to maintain homeostasis. The maintenance of whole-body protein content in organisms involves a highly controlled balance of rates of turnover regulated by synthesis and degradation (Ciechanover, 2005; Ohsumi, 2014; Schoenheimer et al., 1939; Waterlow, 1995, 2006). The requirement for protein renewal through turnover varies considerably with combinations of biological and environmental factors. The rate of protein synthesis and degradation can depend on tissue type, nutritional state, life history stage, environmental conditions and general physiological status (Carter and Houlihan, 2001; Fraser and Rogers, 2007). Growth rate differences have been correlated with different levels of protein turnover, from marine invertebrate species to fish and mammals (Bates and Millward, 1981; Bayne, 2017; Bayne and Hawkins, 1997; Fraser and Rogers, 2007; Hawkins et al., 1986; Waterlow, 2006). Individuals with lower rates of protein turnover show higher growth rates, presumably due to energy trade-offs between protein synthesis, degradation and growth processes (Bayne and Hawkins, 1997). If more energy is allocated to support high rates of protein turnover ('maintenance cost'), then less energy is available for growth. Although the general relationship between growth and protein metabolism has been investigated by manipulating environmental conditions in wild-type animals (e.g. food and temperature; Bayne and Hawkins, 1997; Houlihan, 1991), the biochemical bases of genetic variation in growth are less well understood (Applebaum et al., 2014; Bayne, 2017). Moreover, for developmental forms where growth is rapid, the relationship between growth and protein metabolic dynamics is poorly defined (in energy terms).

Developmental stages of marine invertebrates have long been used to study macromolecule turnover (Davidson, 1976). The small size of developmental stages and their physiological ability to take up dissolved organic substrates added to seawater have allowed for extensive analysis of biosynthesis (Davidson, 1976; Evans et al., 1983). For the study of protein synthesis, radioactively labeled amino acids have been used for trace labeling without altering the composition and size of the intracellular precursor pool (Berg and Mertes, 1970; Fry and Gross, 1970; Marsh et al., 2001; Pace and Manahan, 2006). During embryogenesis of sea urchins, fractional protein synthesis rates (ratio of protein synthesis to whole-body protein content ×100) are high, at ∼50% per day (Berg and Mertes, 1970; Fry and Gross, 1970; Goustin and Wilt, 1981; Marsh et al., 2001; Pace and Manahan, 2006; Pan et al., 2015a). Because no net growth of whole-body protein content occurs during early development before the feeding larval stage is reached (Moran and Manahan, 2004; Meyer et al., 2007; Pace and Manahan, 2006; Pan et al., 2015a), protein synthesis is equal to degradation; hence, approximately half of the total body protein pool is turned over each day. During later growth of larval stages, fractional synthesis rates can exceed 100% (Carter and Houlihan, 2001). At such high rates of protein synthesis during development and growth, the energy cost of protein synthesis alone can account for the utilization of more than 50% of the total ATP pool (Lee et al., 2016; Pace and Manahan, 2006). Additionally, regulation of protein synthesis is a major biochemical response to alter metabolic status in response to environmental perturbation (Pan et al., 2015a; Podrabsky and Hand, 2000, 2015). Given the functional significance of protein metabolism to homeostatic maintenance and metabolic energy turnover, protein synthesis could be used to predict endogenous variation in growth rates – an explicit goal of the present study.

Department of Biological Sciences, University of Southern California, Los Angeles, CA 90089-0371, USA.

*Author for correspondence (manahan@usc.edu)

T.-C.F.P., 0000-0002-1550-4581; D.T.M., 0000-0002-6437-9107

Received 10 October 2017; Accepted 22 March 2018

Experimental cross-breeding of pedigreed lines of the Pacific oyster, *Crassostrea gigas*, is known to produce reproducible growth contrasts among different larval families (Curole et al., 2010; Hedgecock and Davis, 2007; Hedgecock et al., 1995, 2007; Meyer and Manahan, 2010; Pace et al., 2006; Pan et al., 2015b, 2016). In this study, pedigreed lines of *C. gigas* were used to produce larval families that, when reared under similar conditions of food and temperature, showed contrasting growth phenotypes. These larval families were then used to investigate the biochemical bases of growth variation in the context of energy allocation to protein metabolic dynamics.

MATERIALS AND METHODS

Larval culturing

In a series of experimental crosses, a total of 12 larval families were produced by crossing pedigreed lines of adult *Crassostrea gigas* (Thunberg 1793). Four sets of 2×2 factorial crosses were undertaken using different males and females from pedigreed lines developed during a controlled breeding program of up to five generations (ca. 10 years). These pedigreed lines were maintained as separate lines, and the adult broodstock from each pedigreed line was genotyped before being used in an experimental cross to confirm parentage (Hedgecock and Davis, 2007; Sun et al., 2015). The sets of factorial crosses resulted in the production of 16 different larval families. Of these, 12 larval families were selected based on larval numbers (~2 million larvae per family) and phenotypic growth contrasts (Fig. 1). Experimental crosses and larval rearing were conducted in a dedicated marine culture facility at the University of Southern California Wrigley Marine Science Center, located on Santa Catalina Island, CA, USA. Eggs and sperm were removed directly from the gonads of gravid adults. Eggs were fertilized, checked for fertilization success and placed at an initial concentration of 10 eggs ml^{-1} in 200 l culture vessels. Each culture vessel contained 0.2 µm (pore size) filtered seawater at 25°C. A complete replacement of the seawater in each culture vessel was performed every 2 days during all experiments. For each seawater change, continuously flowing ambient seawater was filtered and heated with titanium heat exchangers to the required rearing temperature of 25°C. Temperature data-loggers (HOBO U12, Onset Computer Corp., Bourne, MA, USA) were used to continuously monitor the seawater temperature in individual culture vessels. Over the experimental period tested (up to 17 days, depending on the larval family studied), seawater temperature used to culture larvae was held constant at 24.1±0.90°C (mean±s.d., N=65). When veliger larvae reached feeding competency at 2 days old, larvae in each culture vessel were fed the algae *Isochrysis galbana* at 30 cells μl^{-1}. As larvae grew, the feeding ration was increased to 50 cells μl^{-1} as per standard culture protocols for this species (Breese and Malouf, 1975; Helm et al., 2004).

Growth rate

Growth rates of larvae were measured up to 17 days post-fertilization (rearing duration varied, depending on growth rates of different larval families). Larvae in each culture vessel were sampled at least five times during the growth period studied. At each sampling time point, shell lengths of at least 50 randomly selected larvae were measured on calibrated photomicroscopic images using ImageJ (National Institutes of Health, Bethesda, MD, USA). Larval shell length was quantified as the distance from the anterior to the posterior edge of the shell. Growth rate was calculated for each larval family from the slope of the linear regression model describing the relationship between shell length and age (Fig. 1; Table 1). Preliminary statistical tests comparing different regression methods to analyze growth (shell length) during the larval periods

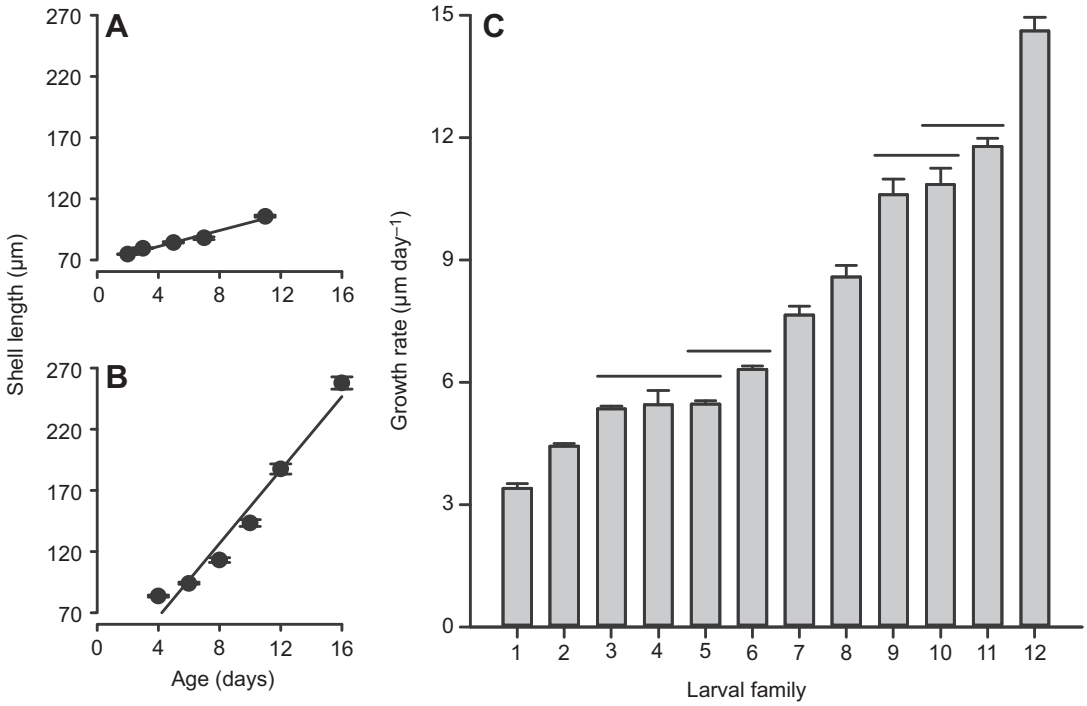

Fig. 1. Growth rate variation between larval families of *Crassostrea gigas*. (A) Family 1 and (B) family 12, representing the minimum and maximum growth rates observed in this study. Values are means±s.e.m. When not visible, error bars are within graphical presentation of the data points. Linear regression models: (A) y=3.4x+67.4, $F_{1,979}$=873.5, r^2=0.47; (B) y=14.6x+10.8, $F_{1,352}$=2010.5, r^2=0.85. (C) Growth rates for 12 larval families produced from crossing pedigreed parental lines of *C. gigas*. Each value represents the slope±s.e. of the linear regression model for a family. Horizontal lines indicate families that are in the same statistical groupings, from Tukey's pair-wise slope comparisons following ANCOVA. See Table 1 for regression models for all 12 larval families.

Journal of Experimental Biology (2018) 221, jeb171967. doi:10.1242/jeb.171967

Table 1. Equations describing relationships between age and shell length, protein synthesis rate, protein content and respiration rate during larval growth of *Crassostrea gigas*

	Shell growth rate			Protein synthesis rate			Protein content			Respiration rate		
	y=shell length (µm)			y=synthesis rate (ng larva^{-1} day^{-1})			y=protein content (ng larva^{-1})			y=respiration (pmol O_2 larva^{-1} h^{-1})		
Family	x=age			x=age			x=age			x=age		
1	$y=3.4x+67.4$	$F_{1,979}=873.47$	$r^2=0.47$	$y=7.305\times e^{0.149x}$	$F_{1,6}=77.84$	$r^2=0.94$	$y=3.911\times e^{0.226x}$	$F_{1,23}=136.60$	$r^2=0.86$			
2	$y=4.4x+63.4$	$F_{1,703}=3389.77$	$r^2=0.83$	$y=24.311\times e^{0.065x}$	$F_{1,6}=6.31$	$r^2=0.56$	$y=5.681\times e^{0.185x}$	$F_{1,26}=682.86$	$r^2=0.97$			
3	$y=5.3x+63.6$	$F_{1,1170}=6458.93$	$r^2=0.85$	$y=25.188\times e^{0.089x}$	$F_{1,9}=41.52$	$r^2=0.84$	$y=12.694\times e^{0.128x}$	$F_{1,34}=261.85$	$r^2=0.89$			
4	$y=5.4x+51.5$	$F_{1,345}=207.31$	$r^2=0.38$	$y=4.606\times e^{0.260x}$	$F_{1,7}=48.01$	$r^2=0.89$	$y=5.201\times e^{0.195x}$	$F_{1,13}=326.31$	$r^2=0.97$	$y=8.254\times e^{0.149x}$	$F_{1,39}=113.25$	$r^2=0.75$
5	$y=5.5x+60.6$	$F_{1,878}=4113.75$	$r^2=0.82$	$y=11.118\times e^{0.149x}$	$F_{1,6}=26.43$	$r^2=0.84$	$y=5.988\times e^{0.192x}$	$F_{1,26}=1342.61$	$r^2=0.98$			
6	$y=6.3x+62.0$	$F_{1,1137}=6792.28$	$r^2=0.86$	$y=30.626\times e^{0.092x}$	$F_{1,11}=21.46$	$r^2=0.68$	$y=13.878\times e^{0.137x}$	$F_{1,35}=355.66$	$r^2=0.91$			
7	$y=7.7x+45.0$	$F_{1,433}=363.82$	$r^2=0.46$	$y=1.632\times e^{0.439x}$	$F_{1,9}=1555.39$	$r^2=0.99$	$y=1.548\times e^{0.339x}$	$F_{1,17}=424.85$	$r^2=0.96$	$y=7.789\times e^{0.125x}$	$F_{1,39}=14.30$	$r^2=0.27$
8	$y=8.6x+47.3$	$F_{1,466}=875.81$	$r^2=0.65$	$y=6.124\times e^{0.248x}$	$F_{1,9}=199.46$	$r^2=0.96$	$y=6.577\times e^{0.218x}$	$F_{1,20}=2772.93$	$r^2=0.99$	$y=6.614\times e^{0.126x}$	$F_{1,45}=147.57$	$r^2=0.77$
9	$y=10.6x+45.7$	$F_{1,486}=2919.29$	$r^2=0.86$	$y=9.642\times e^{0.235x}$	$F_{1,9}=365.06$	$r^2=0.98$	$y=8.043\times e^{0.229x}$	$F_{1,20}=649.79$	$r^2=0.97$	$y=5.051\times e^{0.178x}$	$F_{1,49}=252.19$	$r^2=0.84$
10	$y=10.8x+30.2$	$F_{1,338}=943.40$	$r^2=0.74$	$y=25.764\times e^{0.152x}$	$F_{1,9}=116.72$	$r^2=0.94$	$y=8.624\times e^{0.195x}$	$F_{1,14}=257.89$	$r^2=0.95$	$y=3.402\times e^{0.273x}$	$F_{1,39}=563.19$	$r^2=0.94$
11	$y=11.8x+43.6$	$F_{1,468}=3029.83$	$r^2=0.87$	$y=14.091\times e^{0.232x}$	$F_{1,9}=523.56$	$r^2=0.99$	$y=9.797\times e^{0.225x}$	$F_{1,20}=320.32$	$r^2=0.94$	$y=5.329\times e^{0.232x}$	$F_{1,47}=753.63$	$r^2=0.94$
12	$y=14.6x+10.8$	$F_{1,352}=2010.52$	$r^2=0.85$	$y=30.371\times e^{0.149x}$	$F_{1,9}=109.66$	$r^2=0.93$	$y=7.512\times e^{0.232x}$	$F_{1,14}=912.85$	$r^2=0.99$	$\log(y)=0.134x+0.369$	$F_{1,39}=378.77$	$r^2=0.91$

For shell growth rate, protein synthesis rate and protein content, analyses are based on 12 families; respiration rate analyses are based on seven families (see Results for details).
Values in exponential equations are given to three decimal places for statistical accuracy of calculating differences in protein synthesis, protein content and respiration rates among different larval families.

studied showed that linear regressions of all shell length data within a specific larval family best described growth rate across all 12 families (i.e. lower estimated errors based on higher value of r^2 and smaller residual mean square). A total of more than 7700 individual shell length measurements were conducted for this study. This experimental design of crossing pedigreed lines of *C. gigas* produced a series of larval families that showed a wide range of statistically different phenotypic growth contrasts under similar environmental conditions (Fig. 1C). These phenotypic contrasts were the premise for the study of physiological and biochemical mechanisms that regulate differences in larval growth rates.

Biochemical content

Total protein and lipid content – the two major biochemical components in the larvae of *C. gigas* – were measured in larvae of different shell lengths from different families. Multiple samples (N=3–6), each containing a known number of larvae, were taken from each culture vessel during the growth period studied. A total of 273 protein assays and 98 lipid assays were undertaken in the study. Each sample was immediately placed on ice, then centrifuged in a bench-top mini-centrifuge (2000 ***g***); seawater was then removed and the samples were stored at −80°C pending biochemical analyses. Prior to measurement of protein and lipid content, larvae were freeze-dried to remove any remaining fluids. A known amount (300–400 µl) of deionized water (Nanopure™, Thermo Fisher Scientific, Waltham, MA, USA) was then added to each sample tube, and larvae were sonicated on ice. For protein quantification, larval protein in tissue homogenates was precipitated in ice-cold 5% trichloroacetic acid (TCA), resolubilized in 500 µl of 1 mol l^{-1} NaOH and neutralized with HCl. Protein amounts in each sample were determined using the Bradford dye-binding assay, modified for developing marine invertebrates (Jaeckle and Manahan, 1989; Moran and Manahan, 2004).

For lipid quantification, all lipid classes in larval tissue homogenates were extracted in water:methanol:chloroform (1:1:0.5 v/v); stearyl alcohol was added as the internal standard (Moran and Manahan, 2004). The extraction procedure was followed by phase separation in water:methanol:chloroform (0.9:1:1). The amount of each lipid class in each sample was determined by spotting three replicate samples on different Chromarods™ (1 mm diameter; Iatron Laboratories Inc., Tokyo, Japan). Lipids on each Chromarod were separated using a solvent system containing hexane:ethyl ether (3.5:1) to which 10 drops (Pasteur pipette) of glacial acetic acid were added. Chromarods were dried at 100°C and analyzed with an Iatroscan Flame Ionization Detector system (Iatroscan MK-5, Iatron Laboratories Inc.). The amounts of each major lipid class – phospholipid, triacylglycerol, sterol, free fatty acid and hydrocarbon – were calculated based on extraction efficiency of the stearyl alcohol internal control and known standards of L-α-phosphatidylcholine, tripalmitin, palmitic acid, cholesterol and squalene (all chemicals from Sigma-Aldrich, St Louis, MO, USA). Total lipid content in each larval sample was determined as the sum of the major lipid classes.

Protein synthesis rate

Rates of protein synthesis were determined using the methods developed for larvae of *C. gigas* by Lee et al. (2016). A total of 114 protein synthesis assays (six time points per assay, Fig. S1; i.e. a total of 684 time point samples) were conducted using larvae of different sizes from different families. In each protein synthesis assay, a known number of larvae were incubated in 10 ml of filtered seawater to which 74 kBq [^{14}C]glycine (Perkin-Elmer Inc., Boston,

MA, USA) was added, adjusted to a final concentration of 10 µmol l^{-1} glycine with the addition of non-radioactive glycine ('cold carrier'; Sigma-Aldrich). A series of subsamples was collected every 6 min during a 36 min time-course experiment (Fig. S1). Larvae were placed on a filter membrane (8 µm pore-size; Nucleopore, GE Healthcare, Pittsburgh, PA, USA), gently rinsed with seawater to remove excess radioactivity, and immediately frozen at −80°C until further analysis. The amount of [^{14}C]glycine incorporated into TCA-precipitable proteins at each time point was measured by liquid scintillation counting. This radioactivity was corrected for the change in intracellular specific activity of [^{14}C]glycine in the free amino acid pool of larvae using high-performance liquid chromatography. The total amount of glycine (moles) in each sample was quantified, and the amount of radioactivity (Bq) in the glycine fraction of the chromatographic eluent was determined by scintillation counting to calculate the specific activity of [^{14}C]glycine in the free amino acid pool of larvae (Fig. S1). During these short time-course assays, interconversion of [^{14}C]glycine to other amino acids was minimal (~4%, Fig. S1). The amount of total glycine (moles) incorporated into proteins was converted to the amount of proteins synthesized (grams), based on the mole-percent glycine in proteins for larvae of *C. gigas* (12 ±0.2%) and the average molecular mass of amino acids in proteins (126.6±0.2 g mol^{-1}, calculated from the amino acid composition of hydrolyzed protein) (Lee et al., 2016). For each analysis, protein synthesis rate was calculated from the slope of the linear regression describing the relationship between the amount of newly synthesized proteins and assay time (Fig. S1).

Respiration rate

Respiration rates were measured as described previously (Marsh and Manahan, 1999), with modifications for larvae of *C. gigas* (Pace et al., 2006; Pan et al., 2016). In brief, a known number of larvae (250–500 individuals, dependent on size) were placed in a sealed microbiological oxygen demand respiration vial that contained air-saturated, 0.2 µm (pore size) filtered seawater. For each respiration rate determination, a total of 8–10 replicate respiration vials were used (volume ~600 µl; each vial was independently calibrated for volume). Three control (blank) respiration vials, each containing filtered seawater with no larvae, were included with each set of measurements. Incubation times ranged from 3 to 4 h per assay, depending upon respiration rates (a function of different larval sizes). At the end of the incubation period, the oxygen in each respiration vial was measured by injecting a subsample of seawater into a temperature-controlled microcell (Model MC100, Strathkelvin, North Lanarkshire, UK) that was fitted with a polarographic oxygen sensor (Model 1302, Strathkelvin) and connected to an oxygen meter (Model 782, Strathkelvin). Oxygen sensor readings, corrected for oxygen consumption in the absence of larvae (blanks), were converted to moles of oxygen using standard calibrations.

RESULTS

Growth rate

A total of approximately 24 million veliger larvae, representing 12 different larval families, were produced during the current study. For the larvae in each family, growth rate was calculated from a regression model describing the relationship between shell length and age (e.g. Fig. 1A,B give the primary shell length data for families 1 and 12, as examples of minimum and maximum growth rates). Under similar rearing conditions of food and temperature, larvae of different families had a 4.3-fold difference in growth rates, ranging from 3.4±0.11 (slope±s.e.) to 14.6±0.3 µm day^{-1} (Fig. 1C; slope comparisons of growth rates of all families: $F_{11,7755}$=303.1, P<0.0001, with statistical groupings indicated by horizontal lines). This result shows that the 12 larval families produced by crossing pedigreed lines had contrasting growth phenotypes under similar rearing conditions. Such phenotypic contrasts allowed for further studies of the biochemical and physiological bases of growth variation.

Biochemical content

Whole-body total protein and lipid content are the major biochemical reserves in larvae of *C. gigas* (His and Maurer, 1988; Moran and Manahan, 2004). In the current study, larval protein and lipid content were measured throughout the larval growth period examined (Fig. 2A). During larval growth from 75 to 250 µm (shell length), protein and lipid both increased significantly with shell length, with protein being the dominant biochemical component (average protein-to-lipid ratio of 2.8, N=28). During larval growth, the lipid content of larvae had a higher rate of increase compared with protein content (Fig. 2A; 47-fold and 68-fold increase in protein and lipid, respectively, for a 3-fold increase in shell length; slope comparison for protein and lipid content, $F_{1,367}$=8.26, P=0.004). Although the protein-to-lipid ratio increased during growth, the ratio did not differ among the larval families tested (one-way ANOVA, $F_{6,24}$=1.79, P=0.158). The major lipid classes causing the increase in total lipid content were triacylglycerol and phospholipid (Fig. 2B; slope comparison: $F_{1,192}$=26.26, P<0.0001, i.e. triacylglycerol content increased at a faster rate than phospholipid). In addition to changes in the major lipid classes of triacylglycerol and phospholipid, hydrocarbons, free fatty acids and sterols were also detectable but their amounts did not change during the larval growth period studied (Fig. 2C; family 11 as an example). Combined, those last three classes of lipid accounted for a small percentage (3%) of the total whole-body lipid and protein content of larvae during the growth period studied (Fig. 2C).

Rates of protein synthesis and protein accretion

To understand the dynamics of protein metabolism during growth, an extensive series of *in vivo* measurements was undertaken to measure protein synthesis and accretion in larvae with different growth phenotypes. Rates of protein synthesis were measured (Fig. 3A) and compared with the daily rates of protein accretion (calculated from the relationship between protein content and age for a given family, e.g. Fig. 3B, family 11). Fig. 3C gives the direct comparison of rates of protein synthesis and accretion, allowing the calculation of protein depositional efficiency and protein degradation for larvae of specific shell lengths from each of the different families.

For each determination of the rate of protein synthesis, duplicate time-course assays were conducted using different aliquots of larvae from a given family (Fig. S1). Each set of duplicate assays (a total of 57 sets were completed, i.e. 114 total assays) was in close agreement, with slopes not being statistically different; hence, data from the two assays were pooled to provide a single rate calculation (±s.e. of slope) (Fig. S1F). The rate of protein synthesis in larvae increased with age (Fig. 3A, family 11) – a similar trend to the observed increase in whole-body protein content for this same larval family measured over the equivalent time period [Fig. 3B; exponential equation describing the relationship between protein content and age: protein content (ng $larva^{-1}$)=$9.797\times e^{0.225\times age}$]. Converting protein content to rate of protein accretion for 10 day old larvae from family 11, the daily protein accretion rate was

Journal of Experimental Biology (2018) 221, jeb171967. doi:10.1242/jeb.171967

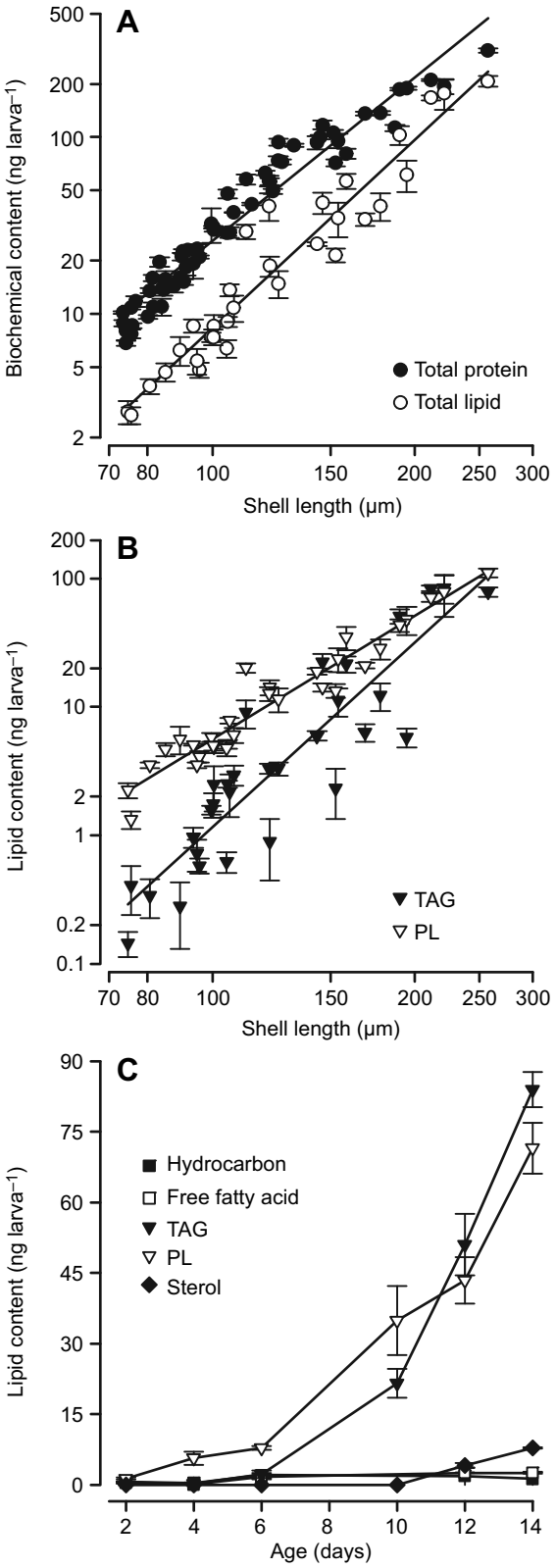

Fig. 2. Changes in lipid classes and protein content during larval growth of *C. gigas*. (A) Total protein content and total lipid content as a function of shell length. Regression models: log(protein)=3.2×log(shell length)−5.0, $F_{1,272}$=3876.5, r^2=0.94; log(lipid)=3.5×log(shell length)−6.1, $F_{1,97}$=1049.5, r^2=0.92. (B) Changes in phospholipid (PL) and triacylglycerol (TAG) as a function of shell length. Regression models: log(PL)=3.1×log(shell length)−5.5, $F_{1,97}$=805.8, r^2=0.90; log(TAG)=4.7×log(shell length)−9.3, $F_{1,90}$=306.0, r^2=0.78. (C) Changes in five lipid classes in larvae (family 11) as a function of age: phospholipid, triacylglycerol, hydrocarbon, free fatty acid and sterol. Values shown are means±s.e.m.; *N*=3–6. When not visible, error bars are within graphical presentation of the data points.

20.9 ng larva^{-1} day^{-1} (Fig. 3B; equation used to calculate protein accretion for a 10 day old larvae: $9.797\times0.225\times e^{0.225\times10}$). This analysis was repeated for larvae of many different shell lengths for all larval families (equations of protein content and age for all families are given in Table 1). A notable result emerged from these analyses, showing that the rates of protein synthesis and accretion increased in parallel with shell length across all 12 larval families tested (Fig. 3C; slope comparison, $F_{1,110}$=3.55, P=0.062, regression equations and statistics given in legend), but with different *y*-axis intercepts (intercept comparison, $F_{1,111}$=242.82, P<0.0001). These analyses revealed that the developmental increase in the rate of protein accretion is the result of a proportional increase in the rate of protein synthesis, and is not driven by changes in depositional efficiency (i.e. the ratio of protein accretion to protein synthesis remains statistically constant during larval growth; Fig. 3C). Quantitatively, this relationship can be illustrated for a mid-sized larva of 150 µm shell length. A larva of this particular size had a protein content of 91.9 ng (calculated from the equation of protein content and shell length in Fig. 2A), a rate of protein synthesis of 128.6 ng larva^{-1} day^{-1} (Fig. 3C) and a rate of protein accretion of 18.2 ng larva^{-1} day^{-1} (Fig. 3C). Combined, these values equate to a rate of protein degradation of 110.4 ng larva^{-1} day^{-1} (128.6–18.2=110.4). Based on these values, changes in protein synthesis, degradation and accretion in relation to whole-body protein content can be calculated. For a 150 µm larva of *C. gigas*, the total amount of whole-body protein increased by 20% (18.2/91.9×100) per day. To achieve this growth rate, a high fractional rate of protein synthesis of 140% (128.6/91.9×100) of whole-body protein content was required per day (i.e. 6% h^{-1}), given the low depositional efficiency of 14% (18.2/128.6×100). This low efficiency indicates a high rate of protein degradation, equating to 120% (110.4/91.9×100) turnover of the whole-body protein content of a growing larva. Clearly, this low efficiency (14%) of protein accretion has important implications for energy metabolism related to growth of larvae (as considered below).

The analyses in Fig. 3C are based on the average for all larval stages and families, resulting in single regression lines for the processes of protein synthesis and accretion. Notably, these processes show a parallel relationship throughout larval growth. Possible changes in the dynamics of protein synthesis and accretion were further examined for early phases of development and for later, rapidly growing larval stages. This analysis revealed two distinct phases of protein metabolism (Fig. 4). The first phase for newly fed larvae of <100 µm shell length was characterized by a slow rate of protein accretion of 3.2 ng day^{-1}, with no significant relationship between protein synthesis and protein accretion [Fig. 4, dashed line: log(protein accretion)=−0.02×log(protein synthesis)+0.50, $F_{1,23}$=0.04, r^2=0.002, P=0.848]. In contrast, the second phase for growing larvae >100 µm in shell length showed a 7-fold increase in the rate of protein accretion driven by increased protein synthesis [Fig. 4, solid line: log(protein accretion)=0.96×log(protein synthesis)–0.81, $F_{1,30}$=65.18, r^2=0.69, P<0.001]. The near-unity slope between protein synthesis and accretion shows that depositional efficiency was constant during this phase of growth for larvae of *C. gigas*. This relationship is in contrast to that of earlier phases of larval development, where protein synthesis increased but protein accretion remained constant.

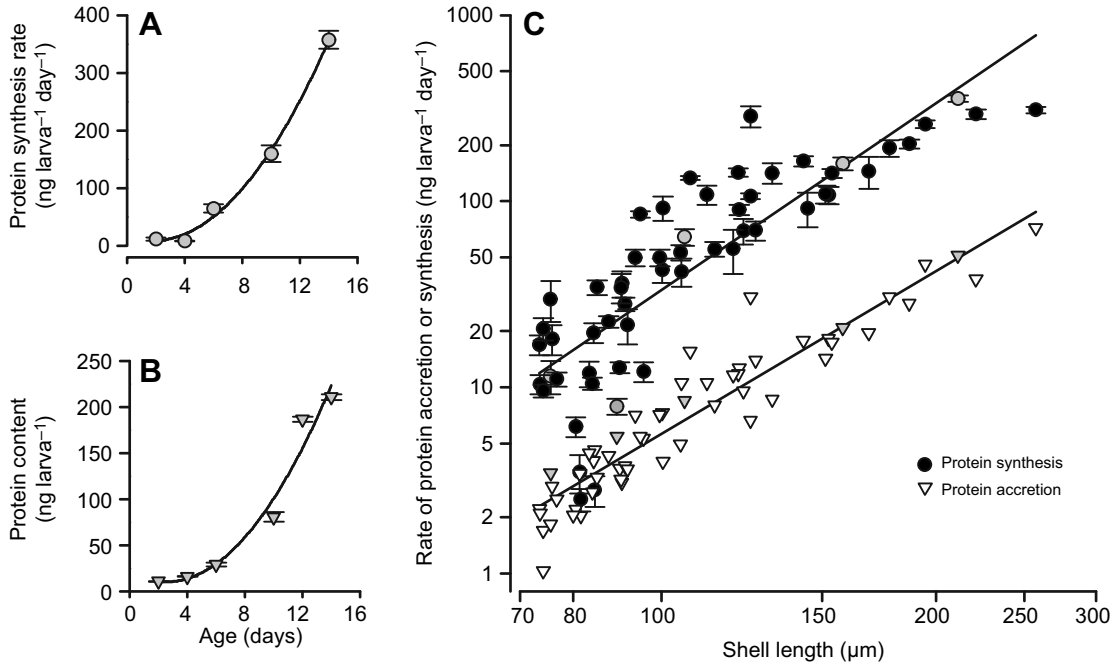

Fig. 3. Rates of protein synthesis and protein accretion during larval growth of *C. gigas*. (A) Protein synthesis rate as a function of age in larvae of family 11. Each data point was calculated from a series of duplicate time-course assays (±s.e. of slope), such as that shown in Fig. S1F. Regression model: $y=14.091\times e^{0.232x}$, $F_{1,9}=523.56$, $r^2=0.99$ ($F_{1,9}$ in this panel is based on a total of $N=10$ protein synthesis assays). See Table 1 for regression models for all 12 larval families. (B) Protein content as a function of age in larvae of family 11. Regression model: $y=9.797\times e^{0.225x}$, $F_{1,20}=320.32$, $r^2=0.94$. Values are means±s.e.m.; $N=3$–6 for each data point. See Table 1 for regression models for all 12 larval families. (C) Rates of protein synthesis and protein accretion as a function of shell length in larvae from 12 families. Synthesis values are slopes±s.e. (gray circles are rates for family 11 from A). Daily protein accretion rates were calculated from the relationship of protein content and age for each family (gray triangles are rates for family 11 from B). Regression models: log(protein synthesis)=3.34×log(shell length)−5.16, $F_{1,55}=132.57$, $r^2=0.71$; log(protein accretion)=2.91×log(shell length)−5.07, $F_{1,55}=449.28$, $r^2=0.89$. The relationships between regressions for protein synthesis and protein accretion are described by parallel slopes (slope comparison, $F_{1,110}=3.55$, $P=0.062$) with different intercepts (intercept comparison, $F_{1,111}=242.82$, $P<0.0001$).

Respiration rate

Rates of oxygen consumption were measured during growth for larvae representing seven different families. For the size range investigated (75–250 µm shell length), on average, respiration increased 29-fold, from 7.4 to 213.2 pmol O_2 larva^{-1} h^{-1} (see Fig. 5 legend for regression equation). For subsequent calculations of changes in the allocation of cellular energy to protein synthesis, the relationship between respiration and age was determined for each family (e.g. Fig. 5 inset for family 11; age–respiration equation for each family is given in Table 1).

Protein turnover and metabolic allocation

A change in the rate of protein synthesis, not a change in depositional efficiency, is the main determinant of protein accretion rate (Figs 3C and 4). Next, a series of calculations was done to determine the biochemical and physiological bases of growth variation across larval families. This calculation was undertaken for an equivalent 8 day growth period for each of the 12 larval families (i.e. 2 to 10 day old larvae; Fig. 6, family 11). The 536 ng total amount of protein synthesized (Fig. 6A, shaded areas) during this period of growth was calculated, starting from the 2 day old first feeding larval stage, and compared with the 80 ng protein accretion in the same 8 day growth period (Fig. 6A, black area). This analysis showed that the average protein depositional efficiency for larvae of family 11 was low at 15% (80/536×100) (Fig. 6A). The total amount of energy consumed as measured by respiration rate (Fig. 5, inset) was then converted to energy equivalents as ATP, and hence joules (Fig. 6B, shaded areas: 2355 µJ) (see Gnaiger, 1983, for general oxyenthalpic equivalents, and Hand, 1999, for interconversion of direct and indirect calorimetry for larvae of *C. gigas* and other species of mollusc). The energy consumed to synthesize the total amount of protein (536 ng) was calculated (1126 µJ) using a value of 2.1±0.2 kJ g^{-1} protein for larvae of *C. gigas* (Lee et al., 2016). Importantly, for this calculation of ATP allocation, the energy cost of protein synthesis is constant – independent of synthesis rate, genotype, growth phenotype and different environmental treatments of food, temperature and seawater pH (Lee et al., 2016; Pace and Manahan, 2006; Pan et al., 2015a). The proportion of the ATP pool (Fig. 6B, black area) required to support the measured rate of protein synthesis for family 11 was 48% (Fig. 6B: 1126/2355×100). A similar analysis of protein synthesis, depositional efficiency and ATP allocation to protein synthesis was undertaken for other larval families showing phenotypic contrasts in growth rates (Fig. 7).

Biochemical bases of differential growth

Regarding the mechanism(s) to support the 4.3-fold faster shell length growth in specific larval families, the analyses revealed that higher growth rates across larval families were explained by higher rates of protein synthesis (slower growing family 1 cf. faster growing family 12: Fig. 7A, $F_{1,11}=25.12$, $r^2=0.72$, $P<0.001$). Depositional efficiency did not change with growth rate on average across all 12 larval families (Fig. 7B, $F_{1,11}=0.07$, $r^2=0.01$, $P=0.794$). However, there were differences in protein depositional efficiency between different families (e.g. Fig. 7B, families 1 and 12). Regarding ATP allocation to protein synthesis across specific larval families showing phenotypic contrasts in the rate of shell growth, a positive relationship was observed between larval family-

Journal of Experimental Biology (2018) 221, jeb171967. doi:10.1242/jeb.171967

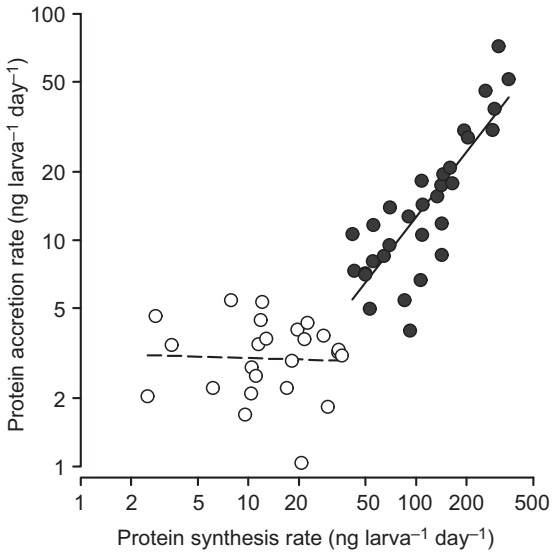

Fig. 4. Protein accretion rate as a function of protein synthesis rate during larval growth of *C. gigas*. The relationship between accretion and synthesis reveals distinct groupings of the rates into an early 'developmental phase' (<100 µm shell length), with constant protein accretion but increasing synthesis [open circles, log(protein accretion)=−0.02×log(protein synthesis)+0.50, $F_{1,23}$=0.04, r^2=0.002], and a later 'growth phase' (>100 µm), showing increases in both protein accretion and synthesis [filled circles, log(protein accretion)=0.96×log(protein synthesis)−0.81, $F_{1,30}$=65.18, r^2=0.69].

dependent shell growth rate and the percent of the ATP pool allocated to protein synthesis (Fig. 7C, $F_{1,6}$=53.42, r^2=0.91, P<0.001). Collectively, these results support the conclusion that protein synthesis is the primary contributor to the variation in growth observed in different larval families (Fig. 1C). Note that there is a predictive relationship between changes in shell length and protein content (see Fig. 2A for equation). This substantially greater investment in protein synthetic capacity to support faster growing

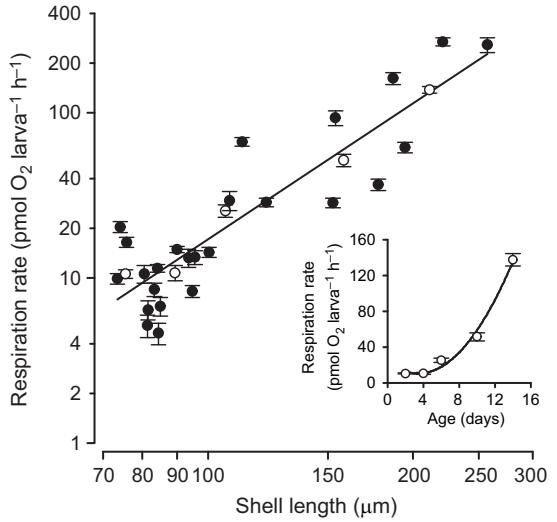

Fig. 5. Respiration rate as a function of shell length during larval growth of *C. gigas* for seven families (families 4 and 7–12). Regression: log(respiration)=2.79×log(shell length)−4.36, $F_{1,303}$=815.84, r^2=0.73. Values are means±s.e.m.; N=8–10 for each data point. Open circles are respiration rates for larvae of family 11 (inset). Inset: respiration as a function of age for larvae from family 11. Regression model: $y=5.329\times e^{0.232x}$, $F_{1,47}$=753.63, r^2=0.94. See Table 1 for regression models for these seven larval families.

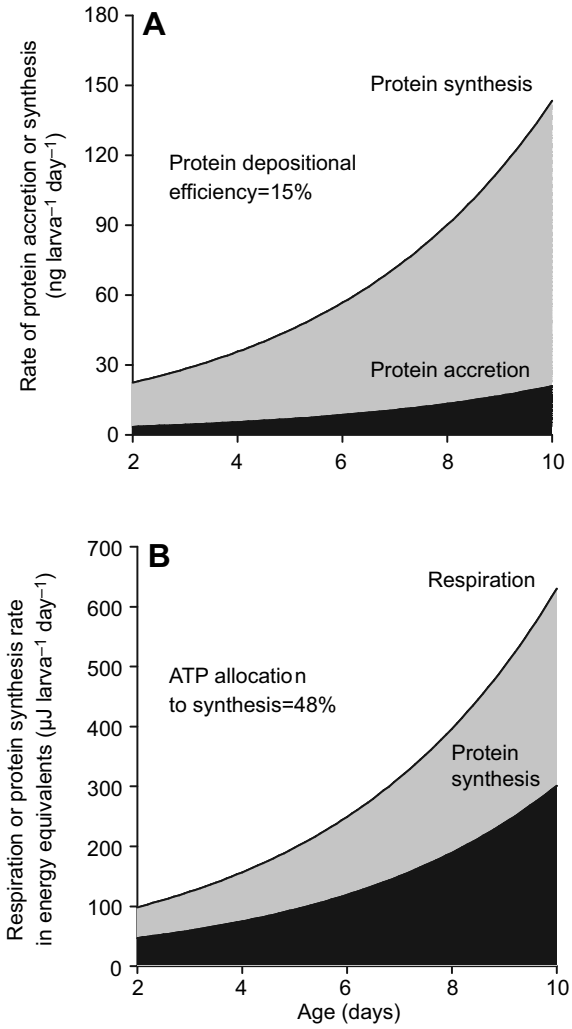

Fig. 6. Calculation of protein synthesis, accretion and metabolic cost of synthesis during larval growth of *C. gigas*. (A) Protein synthesis and accretion rates in larvae from family 11. Lines are based on regression models for protein synthesis (Fig. 3A) and protein content (Fig. 3B) with age. The shaded areas (the combined gray and black areas) represent the total amount of protein synthesized (536 ng per 8 day period) between days 2 and 10; the black area shows the total amount of protein deposited (80 ng) for the same time interval. Based on these values, the average protein depositional efficiency for larvae of family 11 is 15% (the ratio of 80 to 536). (B) Respiration and protein synthesis rates in energy equivalents (see Results for calculations) for larvae from family 11. Values are based on the regression models for respiration (Fig. 5, inset) and protein synthesis (Fig. 3A). The shaded areas (the combined gray and black areas) represent the total amount of available metabolic energy (2355 µJ) between days 2 and 10; the hatched area shows the total amount allocated to protein synthesis (1126 µJ) for the same time interval. Based on these values, metabolic allocation to protein synthesis for larvae from family 11 is 48% (the ratio of 1126 to 2355).

larvae required up to 74% of the total ATP pool to be allocated to this single process (Fig. 7C, family 12). With regard to the ability of larvae to support changes in the 'cost of living' for other ATP-consuming fundamental physiological processes, the limits of bioenergetic trade-offs are discussed below (Fig. 8).

DISCUSSION

Metabolic bases of endogenous variation in growth were investigated in the present study. Controlled crosses of pedigreed genetic lines of the Pacific oyster, *C. gigas*, yielded family-specific

Journal of Experimental Biology (2018) 221, jeb171967. doi:10.1242/jeb.171967

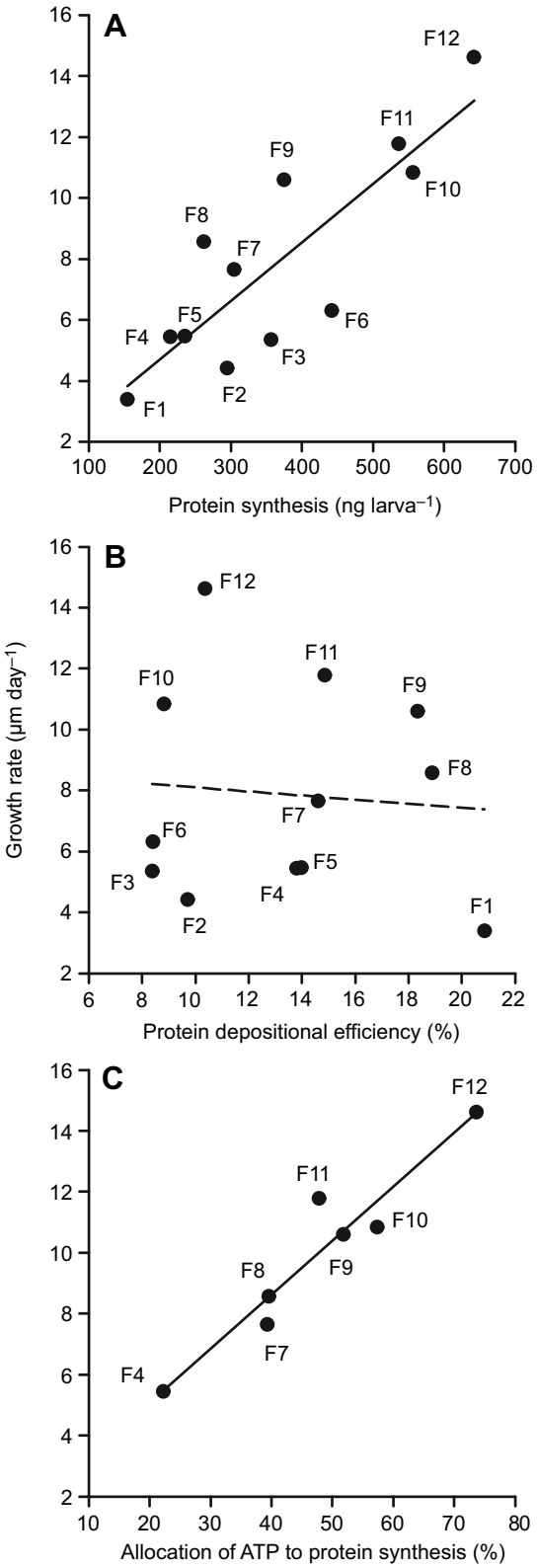

Fig. 7. Analyses of larval family-dependent variation in growth rate, protein synthesis, depositional efficiency and metabolic allocation to synthesis during growth of *C. gigas*. Each value for a given family (with specific family designation, e.g. F1 indicates family 1) represents a calculation as shown in Fig. 6. (A) Relationship between larval growth rate and total protein synthesized between days 2 and 10 for the 12 larval families. Regression model: growth rate=0.02×(protein synthesis)+0.86, $F_{1,11}$=25.12, r^2=0.72. (B) Relationship between larval growth rate and protein depositional efficiency. Regression model: growth rate=−6.67×(protein depositional efficiency)+8.76, $F_{1,11}$=0.07, r^2=0.01. (C) Relationship between larval growth rate and allocation of energy (ATP) to protein synthesis between days 2 and 10 for seven larval families for which respiration rates were measured (Fig. 5; Table 1). Regression model: growth rate=17.72×(allocation of ATP to protein synthesis)+1.53, $F_{1,6}$=53.42, r^2=0.91.

differences in rates of larval shell growth (Fig. 1C). This genetic approach provided phenotypic contrasts in growth rate (Frieder et al., 2017; Pace et al., 2006; Pan et al., 2016), independent of alterations to environmental variables that impact growth and physiology, which are routinely conducted with wild-type animals (e.g. Frieder et al., 2018; Hawkins et al., 1986; Pan et al., 2015a; Podrabsky and Hand, 2000). The protein accretion rate in the fastest growing families was due to increased protein synthesis rate, with a consequence that a greater proportion of metabolic energy was allocated to support higher synthesis (Fig. 7C). This finding suggests that protein synthesis is a potential biomarker for the prediction of growth. The trade-off between increased rates of protein synthesis and increased metabolic allocation to synthesis, within a fixed pool of ATP, could be an important constraint limiting the ability of larvae to respond to other physiological needs. Specifically, a quantitative metabolic allocation model is presented for larval stages of *C. gigas* (Fig. 8) that accounts for the consumption of more than 80% of the total ATP pool by protein synthesis, ion pump activity (Na^+/K^+-ATPase), rates of calcification and protein degradation.

Protein metabolic dynamics underlying growth variation

The study of the dramatic changes in morphological shape and form is a major theme in the field of developmental biology (Gilbert, 2013). Remodeling of body structures during early development requires substantial turnover of the maternally endowed protein content of eggs. Our analyses of the relationship between protein synthesis and accretion revealed a novel finding regarding protein turnover during the transition between early development (differentiation) and subsequent growth of larval forms. This finding is based on the regression models of protein synthesis and protein accretion (Fig. 4) that showed a ‘breakpoint’ for a larva of 100 µm shell length (~6 days old). This regression breakpoint likely represents a shift in the regulatory processes impacting larval growth, when protein synthesis supports a faster rate of protein accretion. Changes in protein synthesis in combination with a low rate of protein accretion during the early phase of larval development indicate high protein turnover likely linked to morphogenesis. During the later larval phase of growth accretion (after ~6 days post-fertilization), the proportional increase in protein synthesis with protein accretion showed a constant protein depositional efficiency of ~14% (ratio of rate of protein accretion to synthesis). For developmental stages of marine invertebrates, a protein depositional efficiency averaging 14% is low compared with that of other species (e.g. in growing sea urchin larvae of two different species, depositional efficiency was ~30%; Pace and Manahan, 2006; Pan et al., 2015a). In general, studies of depositional efficiency in animals show that protein accretion is inefficient (i.e. small amount of accretion relative to synthesis, 6%–50%; Houlihan et al., 1995; Lobley, 2003; Waterlow, 2006; Moltschaniwskyj and Carter, 2010). Additionally, the protein depositional efficiency in larvae of *C. gigas* remained constant, regardless of changes in larval shell length or whole-body protein content. This result is in agreement with the general findings

Journal of Experimental Biology (2018) 221, jeb171967. doi:10.1242/jeb.171967

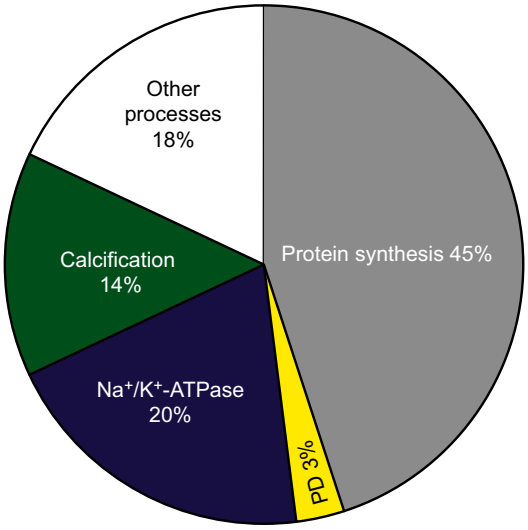

Fig. 8. ATP allocation model for larvae of *C. gigas*. The total area of the pie chart represents the total ATP pool calculated from the respiration rate of a larva of 150 µm shell length. Percent of ATP pool allocated to specific processes are: protein synthesis, 45% (from Fig. 3C, see Discussion for calculations); *in vivo* rates of sodium-potassium transport by Na^+/K^+-ATPase, 20% (from Pan et al., 2016); calcification (shell formation), 14% (from Frieder et al., 2017); protein degradation (PD), 3% (from Fig. 3C and Table 2; see Discussion for calculations). Combined, these components account for 82% of the total available ATP pool. A major part (~15%) of the 18% fraction of the ATP pool that is available for other processes (white section of the pie chart) is likely attributable to the cost of nucleic acid biosynthesis (see Discussion for details).

reported for several species of vertebrates (Carter and Houlihan, 2001; Houlihan, 1991; Houlihan et al., 1995; Waterlow, 2006). Importantly, for all 12 larval families of *C. gigas* analyzed in the present study, increased rates of protein accretion were supported by increased rates of protein synthesis (Figs 3 and 4), i.e. not regulated by changes in rates of protein turnover. Further analysis of the relationship among rates of shell growth (Fig. 1C), rates of protein synthesis (Fig. 7A) and protein depositional efficiency (Fig. 7B) supports the conclusion that endogenous variation in larval growth rate among larval families is the result of variation in rates of protein synthesis, not changes in protein depositional efficiency. Particularly noteworthy is that the phenotypic contrasts of high growth rate require a substantial investment of cellular energy, up to 74% of the total ATP pool (Fig. 7C).

The study of the causes of endogenous growth rate variation during development and growth, even among sibling larvae, has a long history (Strathmann, 1987, and earlier references therein). For adult marine bivalves, it is generally accepted that faster growing individuals have a higher metabolic efficiency with lower rates of protein turnover and lower metabolic rates and, hence, a greater scope for growth (Bayne, 2000, 2004, 2017; Bayne and Hawkins, 1997; Hawkins et al., 1986; Koehn and Gaffney, 1984; Koehn and Shumway, 1982). For developmental stages, the dynamics of protein metabolism that underlie variation in growth rate are less well understood. As with developmental biology, in general (Davidson, 1976; Gilbert, 2013), it is certainly a possibility that the dynamics of protein metabolism differ during rapid growth and development of larvae (Fig. 7) compared with adult stages of the life cycle (Waterlow, 2006). In a previous study (Pace et al., 2006), larval families of *C. gigas* with faster growing phenotypes were shown to require less energy for the same size growth increment than slower growing families raised under the same environmental conditions. Because size-specific respiration rates are constant for larvae of *C. gigas*, and are independent of genotype (Pace et al., 2006; Pan et al., 2016; Fig. 5 in the present study), differences in the cost of growth are dependent upon development time and not on differences in genotype-dependent, size-specific respiration rates. By focusing on protein metabolic dynamics, the prior analysis in Pace et al. (2006) was extended here to show that larvae with faster growth have increased rates of protein synthesis (Fig. 7A). This was achieved with a fixed ATP pool within a given family by allocating more ATP to support the rate of protein synthesis in larval families that have phenotypic contrasts in growth (Fig. 7C). The implications of the metabolic cost of this biochemical strategy are examined below in the context of energy use trade-offs required to support the complex physiological bases of development and growth.

Metabolic energy allocation during development and growth

Biochemical analyses of metabolic regulation and allocation of cellular energy have provided important insights into the hierarchy of ATP-consuming processes (Rolfe and Brown, 1997; Siems et al., 1992). Yet, studies of how organisms maintain adequate turnover of ATP in response to environmental change are still scant (Hochachka and Somero, 2002; Somero et al., 2017). At the level of the whole organism, defining the biochemical and physiological mechanisms that regulate metabolism is challenging because of the complexity of large body sizes. Many animals have a life cycle with small developmental stages that permit a 'cell biological' approach to the study of a whole animal (e.g. Houlihan et al., 1995; Marsh et al., 2001; Pace and Manahan, 2006; Podrabsky and Hand, 2000, 2015). For instance, larvae of *C. gigas* are known to transport amino acids from seawater and rapidly incorporate those precursors into protein (Manahan, 1983), thereby allowing quantitative measurements of protein synthesis rates for larvae at different stages of development and growth in the present study. Combining measurements of rates of protein synthesis with respiration, protein accretion and the metabolic cost of protein synthesis and degradation permits an analysis of ATP production and allocation to specific processes during development and growth.

A model of energy allocation is presented in Fig. 8 for larvae of 150 µm in shell length – representing the approximate mid-point size for the larval phase of *C. gigas*. For larvae of this size, rates of protein synthesis and degradation were 128.6 and 110.4 ng $larva^{-1}$ day^{-1}, respectively (Fig. 3C; see also calculations in Results, 'Rates of protein synthesis and protein accretion'). The corresponding respiration rate for a 150 µm larva was 51.3 pmol O_2 $larva^{-1}$ h^{-1} (Fig. 5). Protein synthesis, degradation and respiration rates were converted to energy equivalents using (i) the measured energy cost of protein synthesis of 2.1±0.2 kJ g^{-1} protein for larval stages of *C. gigas* (Lee et al., 2016), (ii) the estimated energy cost of degradation of 0.14 kJ g^{-1} protein (Table 2), and (iii) an oxyenthalpic value of 484 kJ mol^{-1} O_2 (Gnaiger, 1983). An important premise of this oxyenthalpic calculation is that under normoxic conditions, as used in the present study (Fig. 5), ATP production is fully aerobic (Hand, 1999); hence, measured rates of oxygen consumption represent the oxyenthalpic equivalents of all metabolic pathways of interconvertible energy. The resultant rates in energy equivalents are 270 µJ $larva^{-1}$ day^{-1} (128.6×2.1) for the energy required to support protein synthesis and 15 µJ $larva^{-1}$ day^{-1} for protein degradation (110.4×0.14). The total energy production measured by respiration is 596 µJ $larva^{-1}$ day^{-1} (51.3×24×484/1000) (value corrected for rates per hour, Fig. 5, to rates per day). Hence, 45% (270/596×100) of the total ATP pool is allocated to protein synthesis, whereas only 3% (15/596×100) is required to support the cost of protein degradation.

Table 2. Calculation of the cost of protein degradation in larvae of *C. gigas*

Steps to estimate cost of protein degradation	Calculated value
(1) Average energy cost of protein degradation (DHFR)	65 mol ATP mol^{-1} protein
(2) Molecular weight of dihydrofolate reductase (DHFR)	21,500 g mol^{-1}
(3) Average energy cost of degradation per unit mass of DHFR	0.003 mol ATP g^{-1} protein
(4) Average energy liberated from ATP hydrolysis	45 kJ mol^{-1} ATP
(5) Estimated energy cost of protein degradation	0.14 kJ g^{-1} protein
(6) Measured energy cost of protein synthesis	2.1 kJ g^{-1} protein

(1) Peth et al. (2013) present a set of empirical measurements of the ATP requirement for protein degradation by the 26S proteasome pathway. Based on their findings, an average of 65 ATP molecules are consumed by 26S proteasomes for the degradation of one ubiquitinated protein (dihydrofolate reductase, DHFR). Peth et al. (2013, see their table 1) give a range of 50–80 ATP molecules per protein molecule degraded.
(2) The molecular weight of DHFR without ubiquitin is 21,500 g mol^{-1} (Peth et al., 2013).
(3) Based on 65 ATP molecules per degraded protein (step 1) and the molecular weight (step 2), 0.003 moles of ATP (i.e. 65/21,500) are required for the degradation of 1 g of the protein DHFR. Additionally, Peth et al. (2013) also present the average cost of 130 ATP molecules per protein molecule for the degradation of a larger protein, cyclin-dependent protein serine/threonine kinase inhibiting protein Sic1, of molecular weight 38,000 g mol^{-1}. Based on these two proteins that have an ∼2-fold difference in molecular weight, the calculated degradation cost is the same, at 0.003 mol ATP g^{-1} protein (i.e. 130/38,000) for Sic1 and DHFR.
(4) On average, 1 mole of ATP yields 45 kJ of energy. This value is the average of 30 and 60 kJ mol^{-1} ATP, which encompass the range of energy liberation from ATP hydrolysis under different biological conditions (Bergman et al., 2010; Lehninger, 1975; Ross, 2006).
(5) The average energy cost of protein degradation is estimated to be 0.14 kJ g^{-1} protein (i.e. 0.003×45) per unit mass.
(6) From Lee et al. (2016), the cost of protein synthesis in larvae of *C. gigas* is 2.1±0.2 kJ g^{-1} protein, a metabolic cost that is fixed across genotype, phenotype and environmental temperature.

The molecular biological mechanisms of protein degradation have been studied extensively for decades (Ciechanover, 2005; Ohsumi, 2014; Schoenheimer et al., 1939; Waterlow, 1995, 2006); however, far less is known about the metabolic energy cost of protein degradation (Benaroudj et al., 2003; Peth et al., 2013). Our analysis highlights major potential differences in the metabolic costs of protein synthesis (2.1 kJ g^{-1} protein) and degradation (0.14 kJ g^{-1} protein) in larvae of *C. gigas*, with synthesis being 15-fold more energetically expensive than the estimate for degradation (Table 2). Pending further detailed analysis of the cost of degradation for a range of different proteins by different degradation pathways, this value is presented as a preliminary estimate of the relative costs of protein synthesis and degradation as the basis for constructing an ATP allocation pie chart for a developing animal (Fig. 8). As noted below, the cost of degradation is likely to be around 3% of the ATP pool, given the measured allocation of ATP to the other physiological processes. Although it is possible that other degradation pathways exist in larvae of *C. gigas*, the analysis of ATP use by protein synthesis and ion transport shows that two processes consume the vast majority of the available ATP pool. If additional degradation processes are present in this species, they would consume only a small fraction of the available ATP (i.e. those metabolic costs must 'fit' within the small fraction of the ATP pool available to support other processes, as illustrated in Fig. 8).

A metabolic allocation model based on identified biochemical processes that account for over 80% of the total energy consumption in larvae of *C. gigas* is presented in Fig. 8. Specifically, (1) 45% of ATP is allocated to protein synthesis (this study), (2) 20% to *in vivo* rates of ion transport by Na^+/K^+-ATPase (Pan et al., 2016), (3) 14% to calcification (Frieder et al., 2017) and (4) 3% to protein degradation (this study). For the 18% of the ATP pool that was not accounted for by these calculations, the most likely category of biosynthesis requiring the majority of the remaining fraction of the ATP pool is DNA and RNA synthesis. For example, Siems et al. (1992) reported that nucleic acid biosynthesis can account for ∼15% of the available ATP pool in an isolated mammalian cancer cell line. Another noteworthy conclusion from the ATP allocation model in Fig. 8 is that the cost of lipid synthesis and accretion appears to be small, based on the available fraction of the total ATP pool not accounted for by other known biochemical processes. This suggests that the rapid accumulation of lipids – especially triacylglycerol – during growth of *C. gigas* (Fig. 2B) required minimal energy cost for synthesis.

A major theme of the current study is the application of genetic crosses to produce contrasting phenotypes. In addition to the 4.3-fold variation in rates of larval shell growth (Fig. 1C), it is noteworthy that the allocation of ATP to protein synthesis also varied significantly – from 22% to 74% among different larval families (Fig. 7C). This suggests that the other major ATP-consuming processes must also vary to meet the energy constraint set by the total size of the ATP pool. Indeed, underlying the average of 20% for metabolic allocation to *in vivo* rates of ion transport by Na^+/K^+-ATPase (Fig. 8), there is a substantial range in allocation to this single process among different larval families, varying from 12% to 34% (Pan et al., 2016). For instance, a larval family identified in this study that had the capacity to allocate up to 74% of the ATP pool to protein synthesis alone (Fig. 7C, family 12) may have a correspondingly lower energy demand to support ion transport by Na^+/K^+-ATPase (e.g. 12%, the lowest percentage ATP allocation among larval families reported by Pan et al., 2016). Collectively, these results highlight the importance of further studies to investigate genetically defined variation in trade-offs between major energy-consuming processes and 'fitness traits' related to the allocation of cellular energy in response to environmental change.

Predictions and trade-offs

Differences in growth are central to considerations of larval ecology and recruitment (Cushing, 1990; Houde, 2008; Widdows, 1991). For dispersive phases of larval development, faster growing individuals would appear to have an advantage of completing the planktonic phase in shorter time to advance to the juvenile stages (Hare and Cowen, 1997; Houde, 2008; Rumrill, 1990). Yet, standing genetic variation in growth phenotype is evident in many organisms (Arendt, 1997; Dmitriew, 2011) and in larvae of *C. gigas* (Fig. 1C; also see Pace et al., 2006; Pan et al., 2015b, 2016), suggesting that there is an advantage to maintaining growth variation within a population. The maintenance of growth variation has been attributed to trade-offs among growth rate and other biological traits, such as reproduction, immune function, active metabolism and environmental resilience (Allen et al., 2016; Arnott et al., 2006; Mangel and Stamps, 2001). Additionally, for animals that are selected through breeding programs for increased growth and yield, trade-offs between production traits and sensitivity to temperature have been reported (Sae-lim et al., 2017). Limits in the allocation of ATP at different life history stages are often invoked as possible explanations for such trade-offs. Given the importance of the Pacific oyster, *C. gigas*, in worldwide aquaculture (FAO, 2016), the metabolic trade-offs illustrated for

different larval families in Fig. 7 have important implications for production and yield. These results for larvae of *C. gigas* provide a quantitative analysis of ATP allocation strategies for possible trade-offs related to growth and resilience to environmental stress.

The allocation of ATP to increased rates of protein synthesis explains ∼90% of the variation in larval growth rate (see regression statistics for Fig. 7C). One possible trade-off for supporting the higher costs for growth is that only a small amount of the ATP pool remains for other energy-requiring processes, such as those needed to respond to environmental change and other compounding stressors. Previously, it was shown that growing sea urchins respond to the stress of experimental acidification of seawater by allocating an additional 20% of the fixed ATP pool to support increased rates of protein synthesis and ion transport (Pan et al., 2015a). Combining that finding with the present results for *C. gigas* suggests that faster growing larval families – with a greater allocation of ATP to support protein synthesis – could suffer in rapidly changing environments because of a lack of an ability to allocate ATP in support of other essential cellular functions. Potential alterations to this scenario are genotype-by-environment interactions, where different families of larvae respond differently to environmental change, as proposed by Applebaum et al. (2014) and shown by Frieder et al. (2017) for larvae of *C. gigas*. The approach taken in the present study that combines genetic cross-breeding of pedigreed lines with studies of development and growth facilitates a greater understanding of the biochemical and physiological bases of phenotypic growth variation. In turn, such quantitative analyses of cellular energy trade-offs could facilitate more accurate predictions of adaptive potential to future scenarios of environmental change.

Acknowledgements
Our deep appreciation to Dr Dennis Hedgecock and his laboratory group for advice and genotyping of the parental broodstock used in this study. We thank Taylor Shellfish Farms for their support in maintaining pedigreed lines of the Pacific oyster.

Competing interests
The authors declare no competing or financial interests.

Author contributions
Conceptualization: T.-C.F.P., S.L.A., C.A.F., D.T.M.; Methodology: T.-C.F.P., S.L.A., C.A.F., D.T.M.; Validation: T.-C.F.P., S.L.A., C.A.F., D.T.M.; Formal analysis: T.-C.F.P., S.L.A., C.A.F., D.T.M.; Investigation: T.-C.F.P., S.L.A., C.A.F.; Resources: D.T.M.; Data curation: T.-C.F.P., S.L.A., C.A.F., D.T.M.; Writing - original draft: T.-C.F.P., D.T.M.; Writing - review & editing: T.-C.F.P., S.L.A., C.A.F., D.T.M.; Visualization: T.-C.F.P., D.T.M.; Supervision: D.T.M.; Project administration: D.T.M.; Funding acquisition: D.T.M.

Funding
This work was supported by a grant from the Directorate for Biological Sciences, U.S. National Science Foundation (Emerging Frontiers No. 121220587), and the Waitt Foundation (San Diego, CA, USA).

Supplementary information
Supplementary information available online at
http://jeb.biologists.org/lookup/doi/10.1242/jeb.171967.supplemental

References
Allen, D., Rosenfeld, J. and Richards, J. (2016). Physiological basis of metabolic trade-offs between growth and performance among different strains of rainbow trout. *Can. J. Fish. Aquat. Sci.* **73**, 1493-1506.
Applebaum, S. L., Pan, T.-C. F., Hedgecock, D. and Manahan, D. T. (2014). Separating the nature and nurture of the allocation of energy in response to global change. *Integr. Comp. Biol.* **54**, 284-295.
Arendt, J. D. (1997). Adaptive intrinsic growth rates: an integration across taxa. *Q. Rev. Biol.* **72**, 149-177.
Arnott, S. A., Chiba, S. and Conover, D. O. (2006). Evolution of intrinsic growth rate: metabolic costs drive trade-offs between growth and swimming performance in *Menidia menidia*. *Evolution* **60**, 1269-1278.
Bates, P. C. and Millward, D. J. (1981). Characteristics of skeletal muscle growth and protein turnover in a fast-growing rat strain. *Br. J. Nutr.* **46**, 7-13.
Bayne, B. L. (2000). Relations between variable rates of growth, metabolic costs and growth efficiencies in individual Sydney rock oysters (*Saccostrea commercialis*). *J. Exp. Mar. Bio. Ecol.* **251**, 185-203.
Bayne, B. L. (2004). Phenotypic flexibility and physiological tradeoffs in the feeding and growth of marine bivalve molluscs. *Integr. Comp. Biol.* **44**, 425-432.
Bayne, B. L. (2017). *Biology of Oysters*. London, UK: Elsevier.
Bayne, B. L. and Hawkins, A. J. S. (1997). Protein metabolism, the costs of growth, and genomic heterozygosity: experiments with the mussel *Mytilus galloprovincialis* Lmk. *Physiol. Zool.* **70**, 391-402.
Benaroudj, N., Zwickl, P., Seemüller, E., Baumeister, W. and Goldberg, A. L. (2003). ATP hydrolysis by the proteasome regulatory complex PAN serves multiple functions in protein degradation. *Mol. Cell* **11**, 69-78.
Berg, W. E. and Mertes, D. H. (1970). Rates of synthesis and degradation of protein in the sea urchin embryo. *Exp. Cell. Res.* **60**, 218-224.
Bergman, C., Kashiwaya, Y. and Veech, R. L. (2010). The effect of pH and free Mg^{2+} on ATP linked enzymes and the calculation of Gibbs free energy of ATP hydrolysis. *J. Phys. Chem. B* **114**, 16137-16146.
Breese, W. P. and Malouf, R. E. (1975). *Hatchery Manual for the Pacific Oyster*. Corvallis, Oregon: Oregon State University Sea Grant College Program.
Carter, C. G. and Houlihan, D. F. (2001). Protein synthesis. *Fish Physiol.* **20**, 31-75.
Ciechanover, A. (2005). Proteolysis: from the lysosome to ubiquitin and the proteasome. *Nat. Rev. Mol. Cell Biol.* **6**, 79-87.
Curole, J. P., Meyer, E., Manahan, D. T. and Hedgecock, D. (2010). Unequal and genotype-dependent expression of mitochondrial genes in larvae of the pacific oyster *Crassostrea gigas*. *Biol. Bull.* **218**, 122-131.
Cushing, D. H. (1990). Plankton production and year-class strength in fish populations: an update of the match/mismatch hypothesis. *Adv. Mar. Biol.* **26**, 249-293.
Davidson, E. H. (1976). *Gene Activity in Early Development*. New York: Academic Press.
Dmitriew, C. M. (2011). The evolution of growth trajectories: what limits growth rate? *Biol. Rev.* **86**, 97-116.
Evans, T., Rosenthal, E. T., Youngblom, J., Distel, D. and Hunt, T. (1983). Cyclin: a protein specified by maternal mRNA in sea urchin eggs that is destroyed at each cleavage division. *Cell* **33**, 389-396.
FAO (2016). *The State of World Fisheries and Aquaculture*. Rome, Italy: Food and Agriculture Organization of the United Nations.
Fraser, K. P. P. and Rogers, A. D. (2007). Protein metabolism in marine animals: the underlying mechanism of growth. *Adv. Mar. Biol.* **52**, 267-362.
Frieder, C. A., Applebaum, S. L., Pan, T. C. F., Hedgecock, D. and Manahan, D. T. (2017). Metabolic cost of calcification in bivalve larvae under experimental ocean acidification. *ICES J. Mar. Sci.* **74**, 1-15.
Frieder, C. A., Applebaum, S. L., Pan, T.-C. F. and Manahan, D. T. (2018). Shifting balance of protein synthesis and degradation sets a threshold for larval growth under environmental stress. *Biol. Bull.* **234** (in press).
Fry, B. J. and Gross, P. R. (1970). Patterns and rates of protein synthesis in sea urchin embryos: II. The calculation of absolute rates. *Dev. Biol.* **21**, 125-146.
Gilbert, S. F. (2013). *Developmental Biology*. Sunderland, UK: Sinauer Associates.
Gnaiger, E. (1983). Calculation of energetic and biochemical equivalents of respiratory oxygen consumption. In *Polarographic Oxygen Sensors: Aquatic and Physiological Applications* (ed. E. Gnaiger and H. Forstner), pp. 337-345. New York: Springer.
Goustin, A. S. and Wilt, F. H. (1981). Protein synthesis, polyribosomes, and peptide elongation in early development of *Strongylocentrotus purpuratus*. *Dev. Biol.* **82**, 32-40.
Hand, S. C. (1999). Calorimetric approaches to animal physiology and bioenergetics. In *Handbook of Thermal Analysis and Calorimetry. Vol. 4: From Macromolecules to Man* (ed. R. B. Kemp), pp. 469-510. Amsterdam: Elsevier.
Hare, J. A. and Cowen, R. K. (1997). Size, growth, development, and survival of the planktonic larvae of *Pomatomus saltatrix* (Pisces: Pomatomidae). *Ecology* **78**, 2415-2431.
Hawkins, A. J. S., Bayne, B. L. and Day, A. J. (1986). Protein turnover, physiological energetics and heterozygosity in the blue mussel, *Mytilus edulis*: the basis of variable age-specific growth. *Proc. R. Soc. Lond. B Biol. Sci.* **229**, 161-176.
Hedgecock, D. and Davis, J. P. (2007). Heterosis for yield and crossbreeding of the Pacific oyster *Crassostrea gigas*. *Aquaculture* **272**, 17-29.
Hedgecock, D., McGoldrick, D. J. and Bayne, B. L. (1995). Hybrid vigor in Pacific oysters: an experimental approach using crosses among inbred lines. *Aquaculture* **137**, 285-298.
Hedgecock, D., Lin, J.-Z., DeCola, S., Haudenschild, C. D., Meyer, E., Manahan, D. T. and Bowen, B. (2007). Transcriptomic analysis of growth heterosis in larval Pacific oysters (*Crassostrea gigas*). *Proc. Natl. Acad. Sci. USA* **104**, 2313-2318.
Helm, M. M., Bourne, N. and Lovatelli, A. (2004). *Hatchery Culture of Bivalves: A Practical Manual*. Rome, Italy: Food and Agriculture Organization of the United Nations.
His, E. and Maurer, D. (1988). Shell growth and gross biochemical composition of oyster larvae (*Crassostrea gigas*) in the field. *Aquaculture* **69**, 185-194.

Hochachka, P. P. W. and Somero, G. N. (2002). *Biochemical Adaptation: Mechanism and Process in Physiological Evolution*. Oxford, UK: Oxford University Press.

Houde, E. D. (2008). Emerging from Hjort's Shadow. *J. Northwest Atl. Fish. Sci.* **41**, 53-70.

Houlihan, D. F. (1991). Protein turnover in ectotherms and its relationship to energetics. In *Advances in Comparative and Environmental Physiology*, Vol. 7 (ed. R. Gilles), pp. 1-43. Berlin: Springer-Verlag.

Houlihan, D. F., McCarthy, I. D., Carter, C. G. and Marttin, F. (1995). Protein turnover and amino acid flux in fish larvae. *ICES Mar. Sci. Symp.* **201**, 87-99.

Jaeckle, W. B. and Manahan, D. T. (1989). Growth and energy imbalance during the development of a lecithotrophic molluscan larva (*Haliotis rufescens*). *Biol. Bull.* **177**, 237-246.

Koehn, R. K. and Gaffney, P. M. (1984). Genetic heterozygosity and growth rate in *Mytilus edulis*. *Mar. Biol.* **82**, 1-7.

Koehn, R. K. and Shumway, S. E. (1982). A genetic physiological explanation for differential growth rate among individuals of the American oyster *Crassostrea virginica*. *Mar. Biol. Lett.* **3**, 35-42.

Lee, J. W., Applebaum, S. L. and Manahan, D. T. (2016). Metabolic cost of protein synthesis in larvae of the pacific oyster (*Crassostrea gigas*) is fixed across genotype, phenotype, and environmental temperature. *Biol. Bull.* **230**, 175-187.

Lehninger, A. L. (1975). *Biochemistry: The Molecular Basis of Cell Structure and Function*. New York: Worth Publishers.

Lobley, G. E. (2003). Protein turnover—what does it mean for animal production? *Can. J. Anim. Sci.* **83**, 327-340.

Manahan, D. T. (1983). The uptake and metabolism of dissolved amino acids by bivalve larvae. *Biol. Bull.* **164**, 236-250.

Mangel, M. and Stamps, J. (2001). Trade-offs between growth and mortality and the maintenance of individual variation in growth. *Evol. Ecol. Res.* **3**, 583-593.

Marsh, A. G. and Manahan, D. T. (1999). A method for accurate measurements of the respiration rates of marine invertebrate embryos and larvae. *Mar. Ecol. Prog. Ser.* **184**, 1-10.

Marsh, A. G., Maxson, R. E. and Manahan, D. T. (2001). High macromolecular synthesis with low metabolic cost in Antarctic sea urchin embryos. *Science* **291**, 1950-1952.

Meyer, E. and Manahan, D. T. (2010). Gene expression profiling of genetically determined growth variation in bivalve larvae (*Crassostrea gigas*). *J. Exp. Biol.* **213**, 749-758.

Meyer, E., Green, A. J., Moore, M. and Manahan, D. T. (2007). Food availability and physiological state of sea urchin larvae (*Strongylocentrotus purpuratus*). *Mar. Biol.* **152**, 179-191.

Moltschaniwskyj, N. A. and Carter, C. G. (2010). Protein synthesis, degradation, and retention: mechanisms of indeterminate growth in cephalopods. *Physiol. Biochem. Zool.* **83**, 997-1008.

Moran, A. L. and Manahan, D. T. (2004). Physiological recovery from prolonged "starvation" in larvae of the Pacific oyster *Crassostrea gigas*. *J. Exp. Mar. Biol. Ecol.* **306**, 17-36.

Ohsumi, Y. (2014). Historical landmarks of autophagy research. *Cell Res.* **24**, 9-23.

Pace, D. A. and Manahan, D. T. (2006). Fixed metabolic costs for highly variable rates of protein synthesis in sea urchin embryos and larvae. *J. Exp. Biol.* **209**, 158-170.

Pace, D. A., Marsh, A. G., Leong, P. K., Green, A. J., Hedgecock, D. and Manahan, D. T. (2006). Physiological bases of genetically determined variation in growth of marine invertebrate larvae: a study of growth heterosis in the bivalve *Crassostrea gigas*. *J. Exp. Mar. Biol. Ecol.* **335**, 188-209.

Pan, T.-C. F., Applebaum, S. L. and Manahan, D. T. (2015a). Experimental ocean acidification alters the allocation of metabolic energy. *Proc. Natl. Acad. Sci. USA* **112**, 4696-4701.

Pan, T.-C. F., Applebaum, S. L. and Manahan, D. T. (2015b). Genetically determined variation in developmental physiology of bivalve larvae (*Crassostrea gigas*). *Physiol. Biochem. Zool.* **88**, 128-136.

Pan, T.-C. F., Applebaum, S. L., Lentz, B. A. and Manahan, D. T. (2016). Predicting phenotypic variation in growth and metabolism of marine invertebrate larvae. *J. Exp. Mar. Biol. Ecol.* **483**, 64-73.

Peth, A., Nathan, J. A. and Goldberg, A. L. (2013). The ATP costs and time required to degrade ubiquitinated proteins by the 26 S proteasome. *J. Biol. Chem.* **288**, 29215-29222.

Podrabsky, J. E. and Hand, S. C. (2000). Depression of protein synthesis during diapause in embryos of the annual killifish *Austrofundulus limnaeus*. *Physiol. Biochem. Zool.* **73**, 799-808.

Podrabsky, J. E. and Hand, S. C. (2015). Physiological strategies during animal diapause: lessons from brine shrimp and annual killifish. *J. Exp. Biol.* **218**, 1897-1906.

Rolfe, D. F. and Brown, G. C. (1997). Cellular energy utilization and molecular origin of standard metabolic rate in mammals. *Physiol. Rev.* **77**, 731-758.

Ross, J. (2006). Energy transfer from adenosine triphosphate. *J. Phys. Chem. B* **110**, 6987-6990.

Rumrill, S. S. (1990). Natural mortality of marine invertebrate larvae. *Ophelia* **32**, 163-198.

Sae-lim, P., Kause, A., Mulder, H. A. and Olesen, I. (2017). Climate change and selective breeding in aquaculture. *J. Anim. Sci.* **95**, 1801-1812.

Schoenheimer, R., Ratner, S. and Rittenberg, D. (1939). Studies in protein metabolism. X. The metabolic activity of body proteins investigated with *l*(–)-leucine containing two isotopes. *J. Biol. Chem.* **130**, 703-732.

Siems, W. G., Schmidt, H., Gruner, S. and Jakstadt, M. (1992). Balancing of energy-consuming processes of K 562 cells. *Cell Biochem. Funct.* **10**, 61-66.

Somero, G. N., Lockwood, B. L. and Tomanek, L. (2017). *Biochemical Adaptation: Response to Environmental Challenges, from Life's Origins to the Anthropocene*. Sunderland: Sinauer Associates.

Strathmann, M. F. (1987). *Reproduction and Development of Marine Invertebrates of the Northern Pacific Coast: Data and Methods for the Study of Eggs, Embryos, and Larvae*. Seattle: University of Washington Press.

Sun, X., Shin, G. and Hedgecock, D. (2015). Inheritance of high-resolution melting profiles in assays targeting single nucleotide polymorphisms in protein-coding sequences of the Pacific oyster *Crassostrea gigas*: implications for parentage assignment of experimental and commercial broodstocks. *Aquaculture* **437**, 127-139.

Waterlow, J. C. (1995). Whole-body protein turnover in humans–Past, present, and future. *Annu. Rev. Nutr.* **15**, 57-92.

Waterlow, J. C. (2006). *Protein Turnover*. Wallingford, UK: Centre for Agriculture and Biosciences International Publishing.

Widdows, J. (1991). Physiological ecology of mussel larvae. *Aquaculture* **94**, 147-163.

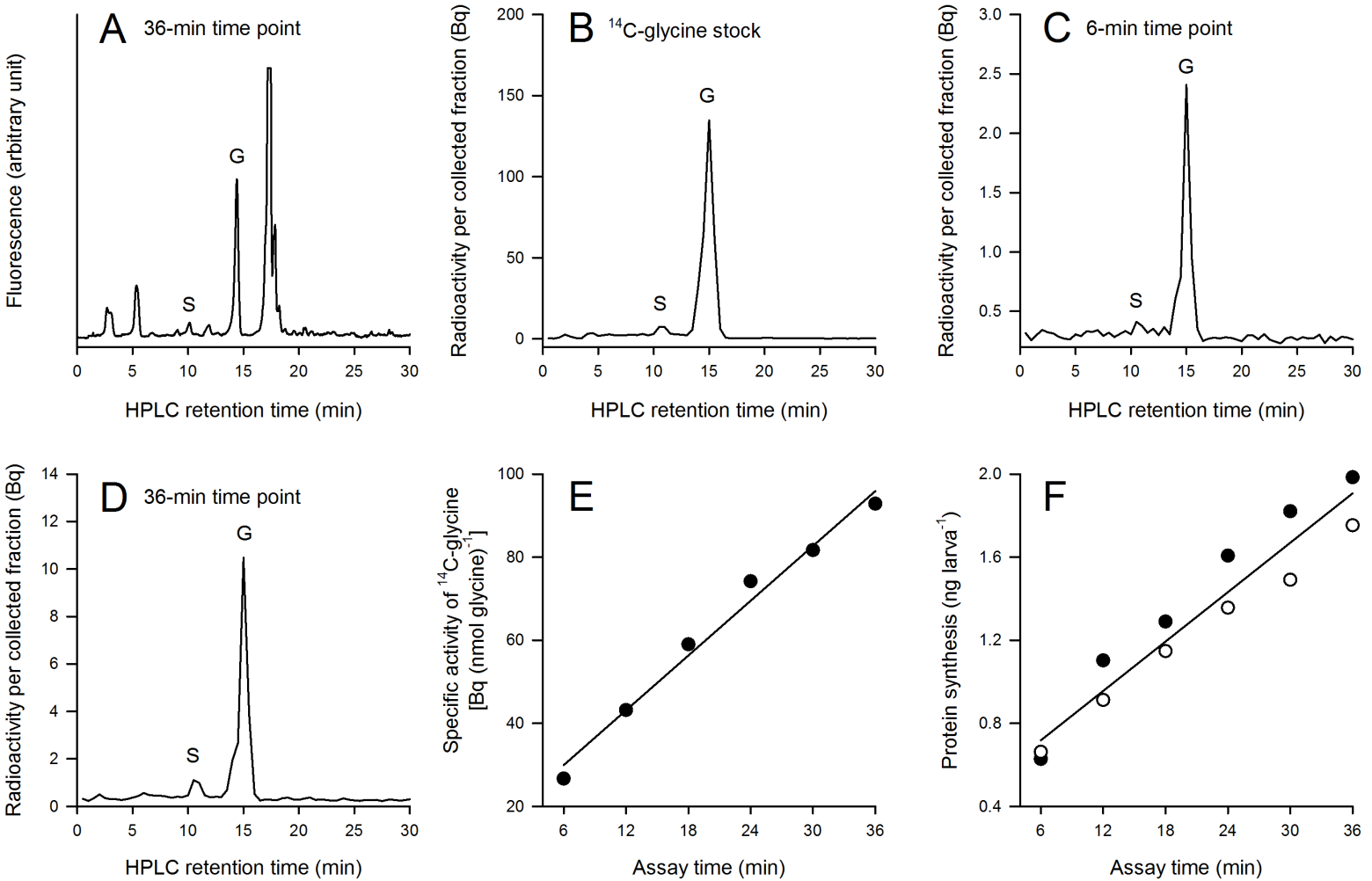
A
36-min time point
Fluorescence (arbitrary unit)
S
G
HPLC retention time (min)
B
14C-glycine stock
Radioactivity per collected fraction (Bq)
S
G
HPLC retention time (min)
C
6-min time point
Radioactivity per collected fraction (Bq)
S
G
HPLC retention time (min)
D
36-min time point
Radioactivity per collected fraction (Bq)
S
G
HPLC retention time (min)
E
Specific activity of 14C-glycine [Bq (nmol glycine)-1]
Assay time (min)
F
Protein synthesis (ng larva-1)
Assay time (min)

Fig. S1. Steps involved in the analysis of protein synthesis rate in larvae of *Crassostrea gigas*.

(A) High-performance liquid chromatography (HPLC) analysis showing the amounts (moles in relative fluorescence units) of free amino acids extracted from 7-d-old larvae of *C. gigas* (Family 6). Labels on peaks are glycine, G, and serine, S. The corresponding analysis of all ^{14}C-labeled amino acids in this sample is shown in panel D.

(B) HPLC analysis for purity of the ^{14}C-labeled glycine stock solution (purchased commercially from Perkin Elmer, Inc.). HPLC eluent was collected continuously throughout the 30 minute analysis using a fraction collector every 30 seconds; each fraction was assayed for radioactivity. ^{14}C-labeled glycine contained 95.4% of the radioactivity, with 4.6% in ^{14}C-labeled serine.

(C) Distribution of ^{14}C-label in the free amino acid pool following a 6-min exposure of larvae to seawater containing the stock solution of ^{14}C-glycine. Note the ratio of radiolabeled glycine and serine present in larvae, is similar to that in the original stock of commercially-supplied ^{14}C-labeled glycine (Panel B).

(D) Distribution of ^{14}C-label in the free amino acid pool after a 36-min exposure of larvae to seawater containing ^{14}C-glycine. The percentage of ^{14}C-label in serine increased slightly to 7.9% at this last, 36-min time point of the protein synthesis assay (see panel E). This represents only a 3.3% (i.e., the difference between 7.9% and 4.6%) interconversion of the original stock of ^{14}C-labeled glycine to ^{14}C-labeled serine during the 36-min assay. Since the mole-percent of serine in whole-body protein of larvae of *C. gigas* is 6.1%±0.1 (Lee et al., 2016) – approximately half of that of glycine, at 12%±0.2 mole-percent – the small percent of ^{14}C-serine in the free amino acid pool has a minimal effect on the calculation of protein synthesis rate.

(E) Specific activity of ^{14}C-glycine in the precursor pool of free amino acids in larvae sampled at different time points during a 36-min time-course assay. Specific activity of glycine [ratio of ^{14}C-labeled (Bq) glycine to total glycine (moles)] was calculated for each of the six different time points using, for example, the moles of total glycine (36 min, panel A) and the corresponding amount of ^{14}C-labeled glycine present in larvae at a given time point (36 min, panel D). Change in the specific activity of ^{14}C-glycine was used to correct the total amount of glycine that was incorporated into protein. Regression: Specific activity = 2.20×time + 16.77, N=6, r^2=0.98, P<0.001.

(F) Duplicate time-course assays to measure protein synthesis rates in 7-day-old larvae. For each synthesis rate, two time-course assays were conducted using different aliquots of larvae from the same larval culture (open and closed circles represents duplicate time-series assays). By comparison of slopes of the two different regressions shown, the rates were not statistically different (P=0.06). Data points were pooled to calculate a single rate of protein synthesis for larvae of this size and age (i.e., corresponding to one data point, as shown in Fig. 3C). Regression: Protein synthesis = 0.04×time + 0.48, N=12, r^2=0.92, P<0.001.